Supporting information

A New Green Titania with Enhanced NIR Absorption for Mitochondria-Targeted Cancer Therapy

Juan Mou, Tianquan Lin, Fuqiang Huang, Jianlin Shi and Hangrong Chen✉

Supplementary figures

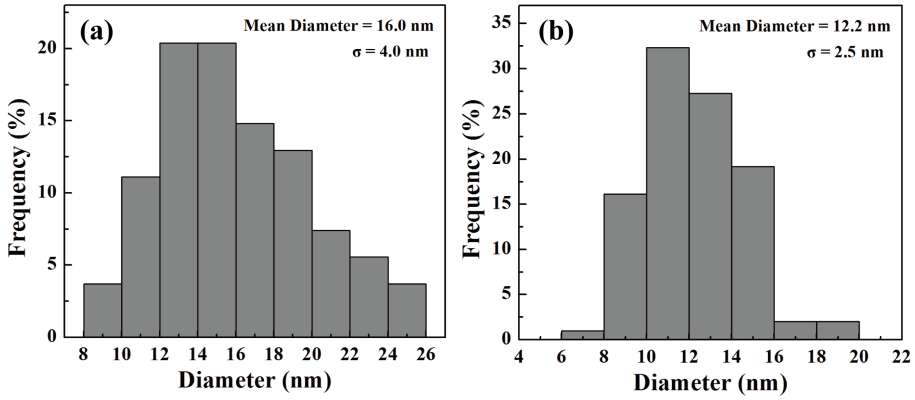

Figure S1. Nanocrystal size distribution histograms of *B*-TiO_{2-x} (a) and *G*-TiO_{2-x} (b).

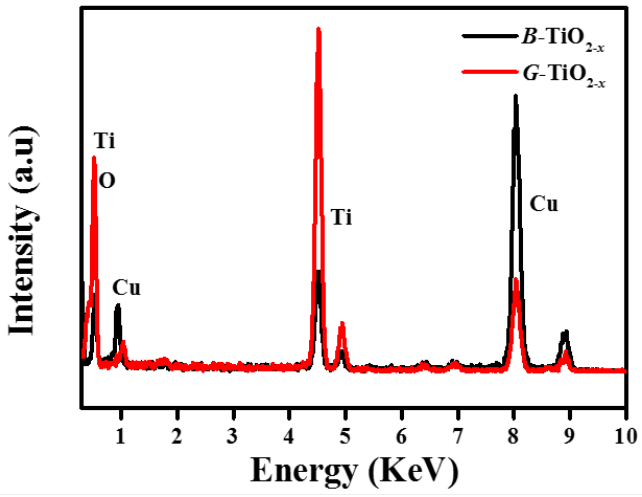

Figure S2. Energy dispersive X-ray spectrum of the as-synthesized *B*-TiO_{2-x} and *G*-TiO_{2-x}.

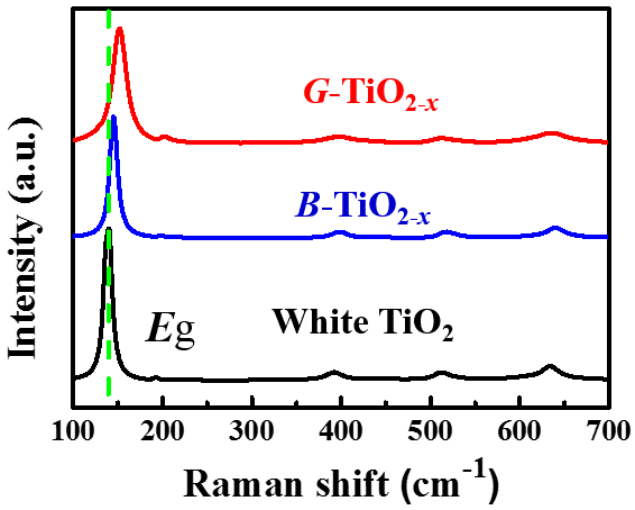

Figure S3. Raman spectra of white TiO_2, as-synthesized *B*-TiO_{2-x} and *G*-TiO_{2-x}.

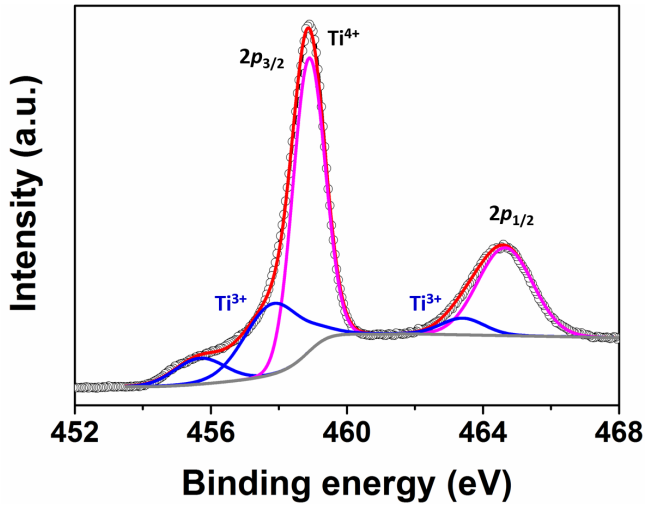

Figure S4. X-ray Photoelectron Spectroscopy spectra of the *G*-TiO_{2-x}. The shoulder peaks (in blue) at ~457 eV in the Ti $2p_{3/2}$ and at 463 eV in Ti $2p_{1/2}$ XPS spectra are correlated with Ti^{3+} while the main peak (in magenta) at 458.9 and 464.6 eV corresponding to Ti $2p_{3/2}$ and Ti $2p_{1/2}$ of Ti^{4+}, respectively.

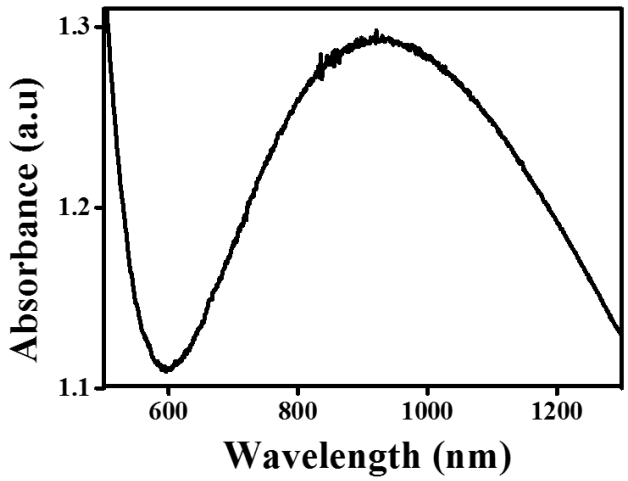

Figure S5. UV-vis absorbance spectrum of aqueous solutions containing *G*-TiO_{2-x} (Ti concentration: 50 ppm).

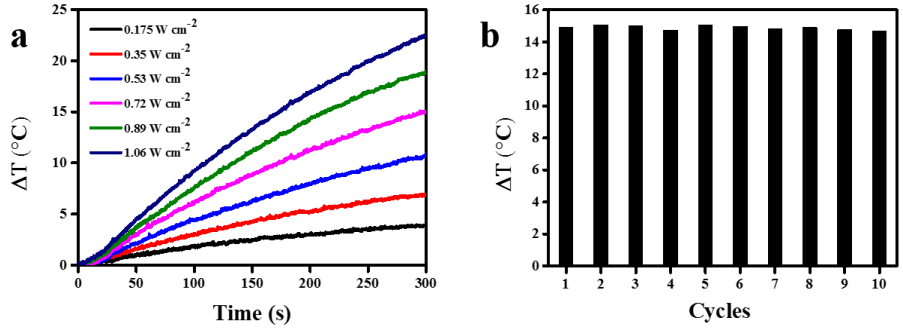

Figure S6. (a) Temperature elevation of the aqueous solution containing *G*-TiO_{2-x} at determined Ti concentration (2 mL, 50 ppm) as a function of irradiation time and power densities (980 nm). (b) Photothermal stability investigation after laser irradiation for 10 cycles (980 nm, 0.72 W cm^{-2}, 5 min).

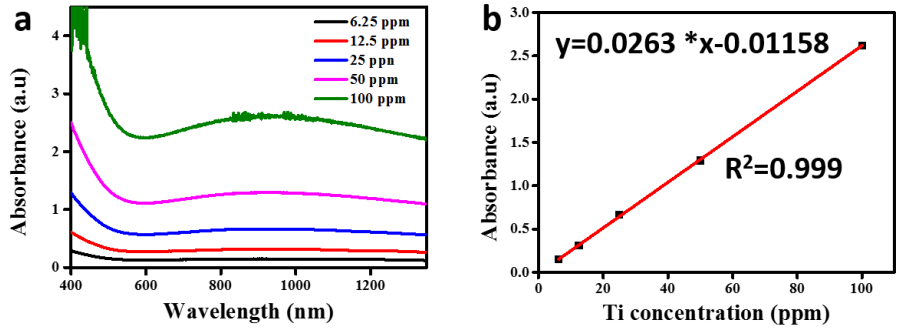

Figure S7. (a) UV-vis absorbance spectra of aqueous solutions containing *G*-TiO_{2-x}-TPP at varied concentrations and (b) the corresponding linear plot of absorbance *vs* concentrations at 920 nm.

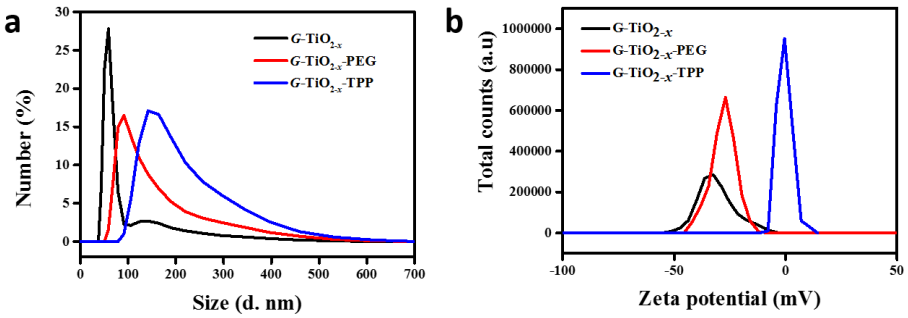

Figure S8. Hydrodynamic diameter distribution (a) and Zeta potential (b) of the as-synthesized *G*-TiO_{2-x} and after PEG, TPP modification.

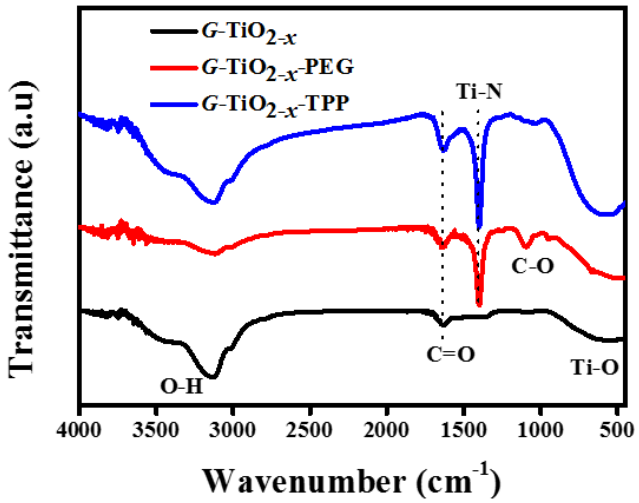

Figure S9. FT-IR spectra of the *G*-TiO_{2-x} and after PEG, TPP modification.

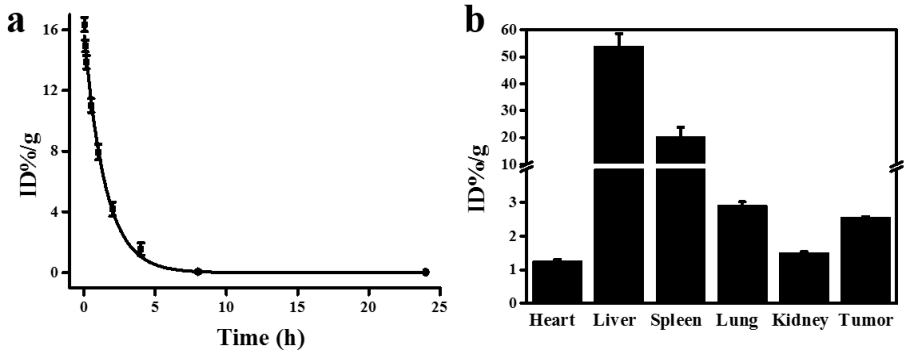

Figure S10. (a) Pharmacokinetic profile of *G*-TiO_{2-x}-TPP following intravenous administration. (b) Biodistribution of *G*-TiO_{2-x}-TPP at 24 h after intravenous injection in mice. Each experiment was repeated three times in triplicate. Data were shown as the means ± SD.

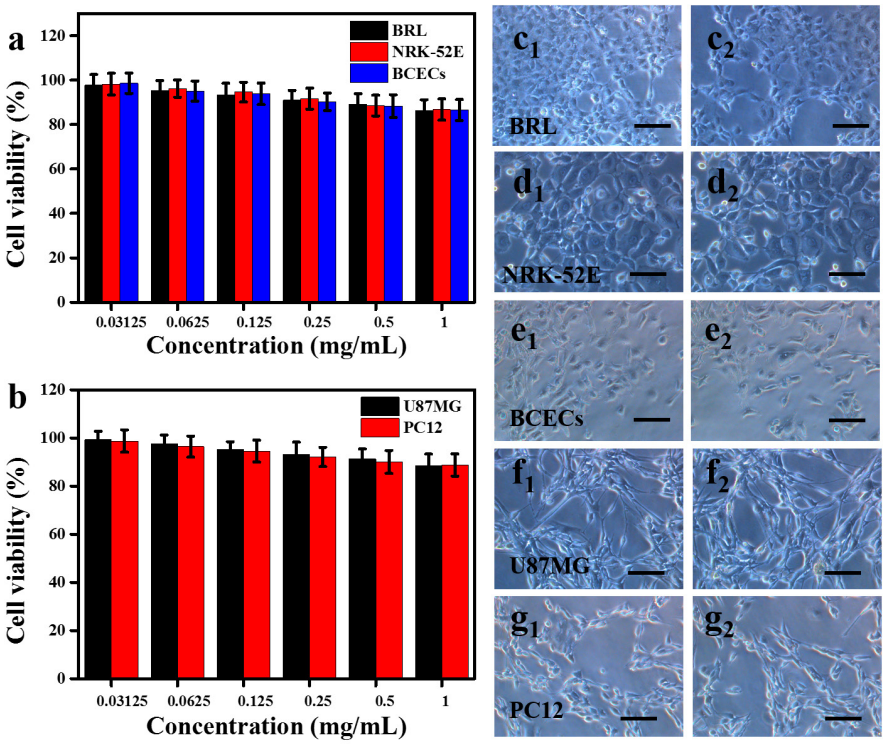

Figure S11. *In vitro* cell viabilities of three types of normal cells (BRL, NRK-52E, BCECs) and two types of brain-related cancer cells (U87MG and PC12) incubated with *G*-TiO_{2-x}-TPP at different concentrations for 24 h, evaluated by a standared MTT assay. Correspongding optical microscopic images of the *in vitro* cell morphology of five types of cells incubated without (c_1-g_1) or with *G*-TiO_{2-x}-TPP (c_2-g_2) (Ti concentration:100 ppm) for 24 h. Each experiment was repeated three times in triplicate. Data were shown as the means ± SD. All the scale bars in (c-g) are 100 μm.

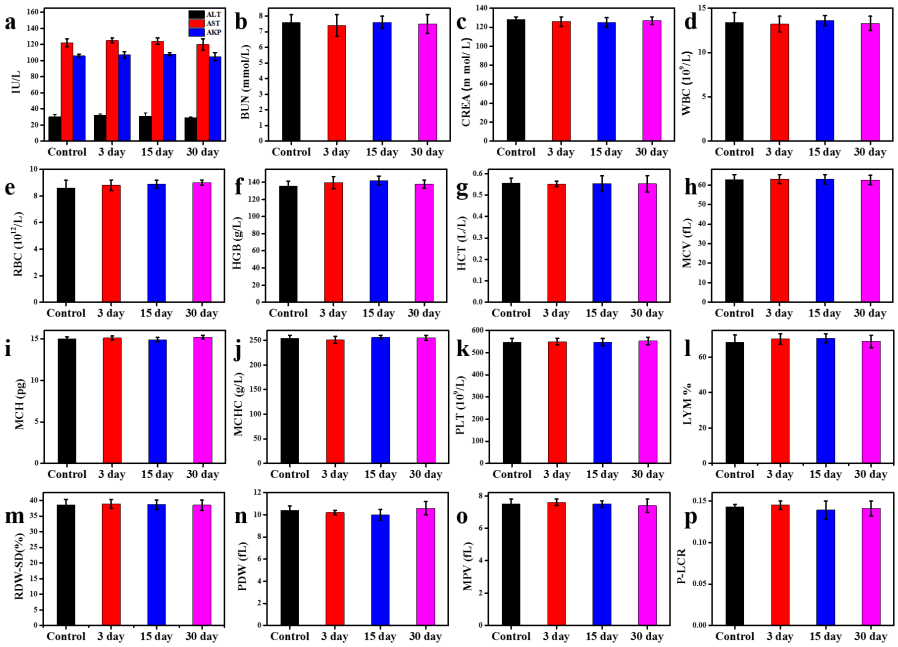

Figure S12. The variations of blood indexes of Kunming mice after intravenous injection of physiological saline (control) or *G*-TiO_{2-x}-TPP (8 mg Ti/kg) at different time points (*i.e.*, 0, 3, 15, 30 days). Each experiment was repeated three times in triplicate. Data were shown as the means ± SD.

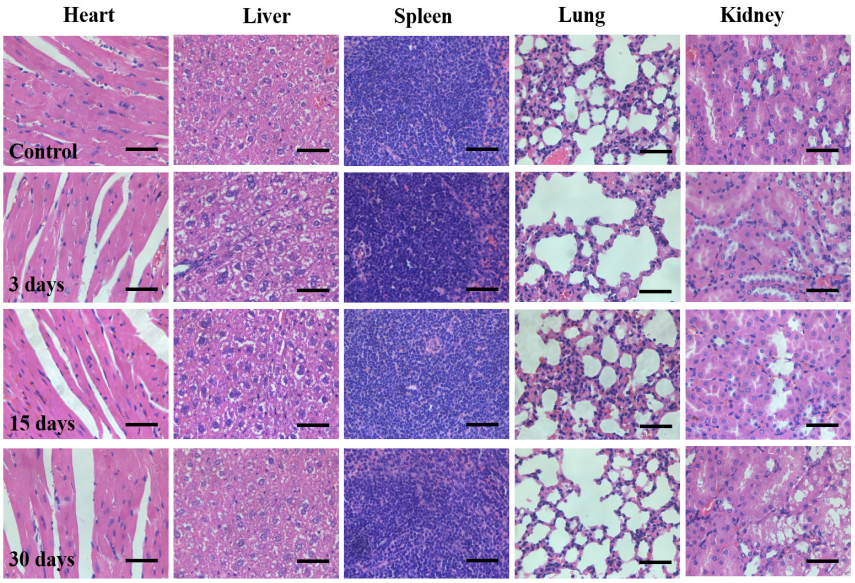

Figure S13. Time courses of histological changes in main organs of Kunming mice *via* H&E staining after intravenous injection of physiological saline (control) or *G*-TiO_{2-x}-TPP (8 mg Ti/kg) at different time points (*i.e.*, 0, 3, 15, 30 days). All the scale bars are 50 μm.

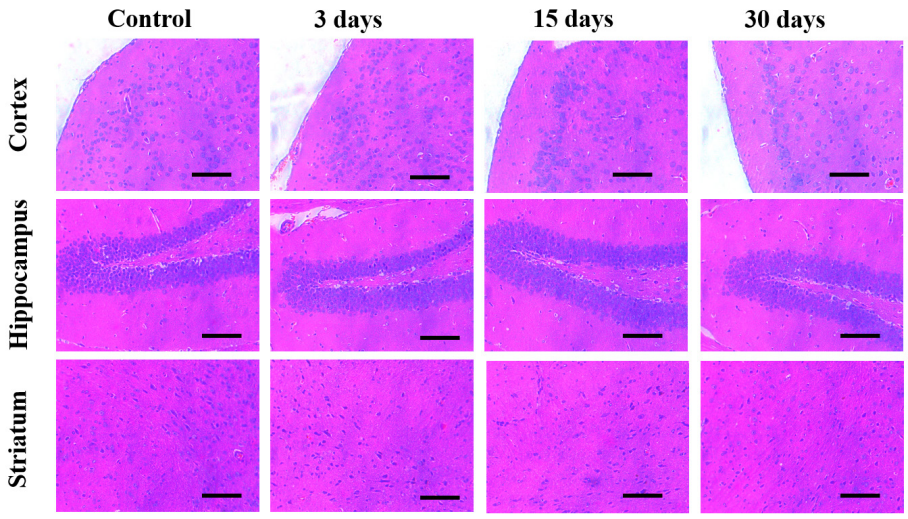

Figure S14. *In vivo* brain toxicity evaluation of *G*-TiO_{2-x}-TPP. H&E-stained main brain tissues sections of cortex, hippocampus and striatum, which were collected from mice treated with intravenous injection of physiological saline (control) or *G*-TiO_{2-x}-TPP (8 mg Ti/kg) at different time points (*i.e.*, 0, 3, 15, 30 days), to monitor the histological changes. All the scale bars are 50 μm.